University of Ottawa

M. Sc. Physics Thesis

MEASUREMENT OF RADIOACTIVE CAESIUM ISOTOPES BY ACCELERATOR MASS SPECTROMETRY

Author:

Cole MacDonald

Supervisor:

Dr. Liam Kieser

Co-Supervisor:

Dr. Jack Cornett

November 13, 2014

Abstract

The first measurements of the radioactive ^{135}Cs and ^{134}Cs isotopes were made on an accelerator mass spectrometer. The natural Ba interference was suppressed using an isobar separator for anions (ISA) in order to measure the less abundant isobaric ^{134}Cs and ^{135}Cs isotopes. It was found that the Ba interference could be suppressed by a factor of 2×10^5 while 25% of Cs was transmitted. Furthermore, through comparing the known natural abundance of Ba isotopes to the measured concentration in a sample it was shown that the ISA does not introduce significant mass dependant fractionation at the level of 0.8%. A slow sequential injection analysis technique was developed to measure ^{135}Cs using ^{134}Cs as a reference isotope. This technique also permitted the monitoring of Ba interference. The ionization efficiency of Cs when analyzed in the molecular anion form, CsF_2^-, was on the order of 10^{-7} while the total measurement efficiency was 1.7×10^{-9}. The abundance sensitivity of this system was found to be ^{135}Cs/ ^{133}Cs $= (1.3 \pm 1.7) \times 10^{-10}$, corresponding to a 3σ detection limit of 132.5 pg of analyte per target. Lastly, using the developed AMS techniques, beta spectroscopy, gamma spectroscopy, and isotope production, a measurement of the half life of ^{135}Cs was made. The two measurements of the half life of ^{135}Cs were 0.72 ± 0.32 Ma and 0.99 ± 0.42 Ma.

Acknowledgements

I would like to thank my supervisors; Dr. Liam Kieser and Dr. Jack Cornett, as well as the University of Ottawa AMS members, Drs. Chris Charles, Xiaoei Zhao, Ted Litherland. Your collective knowledge, guidance, and patience encouraged me to take full advantage of the opportunities these studies granted me. I very much look forward to working with you in the future. I would also like to thank Drs. Robillard and Van Hoof at AECL Chalk River Laboratories for supplying the much needed ^{135}Cs sample as well as Kathy Nielsen at the Royal Military College for assisting the preparation of the ^{134}Cs sample. My thanks to the Natural Sciences and Engineering Research Council of Canada (NSERC) and The Canada Foundation for Innovation (CFI) for funding this research. The Isobar Separator for Anions was designed and supplied by Isobarix and Ionics Mass Spectrometry Group in Bolton, Ontario, Canada, this project would not have been so successful without their contribution, many thanks.

My accomplishments are due, in large part, to the massive contribution and encouragement from my friends and family. My parents, Alan and Leigh MacDonald, could not have expressed more support and encouragement throughout my studies. Thank you both very much for everything you have afforded me.

Statement of Originality

Chapter 3: Barium Suppression and Development of Measurement Techniques

The concept of accelerating the sample Cs as a fluoride superhalogen anion was outlined in previous work done by Dr. Xiaolei Zhao et al. These methods were developed before I began the thesis work. I tested other measurement techniques (various initial anions, operating parameters, target compositions etc.) however none of the tests proved more effective than the procedures that were already in place for measuring Cs. This majority of this work was largely qualitative so I did not included in the thesis.

Tests had not been done prior to my work involving Cs in solution. Only CsF powder had been used for target creation. Therefore, new procedures needed to be developed. I was aided by Dr. Chris Charles in the development the sample preparation and target creation procedures. Once these procedures were in place, however, no further aid was given in experimental sample creation other than requested supervision while I worked with particularly radioactive samples or other hazardous materials.

In order to measure Cs, samples with high abundance of the desired isotopes were needed. I calculated the required exposure time of the $CsCO_3$ to achieve the required amount of ^{134}Cs without ^{135}Cs contamination. The neutron activation of $^{133}CsCO_3$ was done by the Royal Military College (RMC) Slowpoke facility (Kingston, Ontario, Canada). The ^{135}Cs sample (in the form of a pipe section) was sent to Dr. Cornett from Atomic Energy of Canada Limited (AECL) (Chalk River, Ontario Canada). Dilutions of these samples were done with the aid of Dr. Jack Cornett.

The thesis goes on to describe isobaric attenuation of barium and detection of Cs. All of the data presented in these paragraphs were collected and analyzed without aid. This includes all manipulations of the isobar separator and accelerator mass spectrometer components in obtaining the suppression curves and natural abundance measurements of barium as well as the measurements of various Cs isotopes.

Chapter 4: Measurement of Caesium by AMS

All of the data presented in this chapter was collected without aid. The sample preparation was accomplished as described in the previous section. The procedures were developed with the aid of Drs. Charles and Zhao and all the experimental sample preparation was done alone or with supervision if necessary.

While I collected the first data showing unexpected interference after the suppression of barium, it was Dr. Zhao who identified it as Zn dimers and suggested a method of suppressing the molecular interference. Dr. Zhao and I experimentally found the optimal stripper gas pressure to eliminate the Zn dimer interference.

Chapter 5: Half Life Measurement

The ^{134}Cs and ^{135}Cs samples were produced, as mentioned previously, by RMC and AECL respectively. Dr. Cornett and I did the dilutions of these samples. In order to quantify the amount of activity in the samples, they were analyzed by beta and gamma spectroscopy. I performed the beta spectroscopy while the gamma spectrometry of the ^{134}Cs and ^{135}Cs was done by RMC personnel and Dr. Cornett respectively. The analysis of all these spectra was done alone.

Dr. Cornett and I developed the protocol for purifying the Cs samples with AMP while the actual purification and analysis was done myself.

In summary, while aid was given in the development of new protocols/procedures (sample purification, sample preparation, target creation, measurement techniques, etc.), all of data presented in this thesis were collected and analyzed myself, save for the gamma spectrometer measurements of the Cs samples, which were collected by and Dr. Cornett and RMC personnel. (Figures 5.1 and 5.3 in the thesis)

Contents

List of Abbreviations

AMP ..... Ammonium 12-molybdophosphate

AMS ..... Accelerator mass spectrometry

au ..... Arbitrary units

ESA ..... Electrostatic analyzer

FC ..... Faraday cup

GIC ..... Gas ionization chamber

ICPMS ..... Inductively coupled mass spectrometry

ICPMS-QQQ Triple quadrupole inductively coupled mass spectrometry

ISA ..... Isobar separator for anions

LSC ..... Liquid scintillation counting

MS ..... Mass spectrometry

RMC ..... Royal Military College

TIMS ..... Thermal ionization mass spectrometry

List of Tables

List of Figures

Chapter 1

Introduction

1.1 Radioisotopes and Their Detection

Following the substantial advancements of knowledge concerning the atom in the 19th century, experiments unveiling the structure of the atom began emerging. The cumulative efforts of many scientists including J. J. Thompson, Marie Currie, Ernest Rutherford, Frederick Soddy, Neils Bohr, and James Chadwick have lead to a comprehensive understanding of the periodic table. It was found that atoms are not elementary particles, but rather are made up of subatomic particles including protons, neutrons, and electrons. Together, these particles were found to dictate the characteristics of the atom. The number of protons determined the chemical nature of the atom, an excess or lack of electrons determines the overall charge of the atom, and the neutrons aid in the stability of the nucleus.

Experiments done in the 20th century unveiled the concepts of nuclear stability and radioactivity. It was also discovered that atoms of different masses could occupy the same location on the periodic table. These atoms were called isotopes. However, in general, only a few of these isotopes maintain nuclear stability while others undergo radioactive processes to attain a more energetically favourable state. When the process

of radioactive decay occurs the isotope emits characteristic particles and, depending on the method of decay, can change the chemical nature of the atom, shifting its position on the period table.

Analysis of these isotopes was quite difficult, as they could not be separated chemically. Therefore, new methods of separation and detection techniques needed to be developed. This was accomplished by exploiting the two principle differences of isotopes, their characteristic radiation and mass. The particles given off through decay are generally alpha (helium nucleus), beta (electron or positron), or gamma (photon) particles and can be measured using a corresponding spectrometer which separates the particles by energy. This process works well for isotopes with short half lives, but sometimes isotopes can be extremely long lived or even stable. Mass spectrometry resolves this problem by separating isotopes from each other based on their mass.

The combination of these measurement techniques generated an abundance of new information regarding isotopes such as natural abundances and well defined half lives. Furthermore, it was observed that environmental and temporal processes can alter the relative abundance of isotopes through isotopic fractionation and radioactive decay. Accordingly, by analyzing isotopic ratios, the processes themselves could be observed in detail. Applications requiring the quantification of isotopic ratios are numerous; some notable examples include carbon dating, the comparison of the ^{14}C and ^{12}C ratio in an organic material to the isotopes' known natural abundance to deduce its age, or deducing a source of water through the observation of ^{18}O and ^{16}O ratios.[6, 7]

1.2 Mass Spectrometry

Every type of mass spectrometer for isotopic analysis requires three components to analyze a sample: a source that generates a beam of ions, mass filters to separate the beam of ions and a detector to quantify the beam.

A thermal ionization mass spectrometry (TIMS) source consists of a metal filament, most commonly Re or Ta, on which a liquid sample is suspended. After drying, the heated filament begins to thermally ionize the atoms in the sample. The sample atoms, vapourized and ionized by the hot filament, are focused and accelerated out of the source into the mass analysis section. There are many variations in how a beam can be separated as well as the number of separation steps in the analysis. The simplest method of mass separation is to pass the beam through a curved electromagnet. The mass spectrum generated from the magnet can then be analyzed in a number of ways. A Faraday cup (FC) is used to analyze large ion currents. By focusing the sample ion flux into an FC while varying the magnetic field of the electromagnet, a relationship of current vs. magnetic field, and by extension current vs. mass, may be obtained. Alternatively, the magnetic field can be focused into an array of FCs lying on the magnet focal plane. This produces a discrete mass spectrum across a smaller range than the former method. For smaller ion currents, an electron multiplier detector can be used. The ion currents or counts from the analysis of the beam directly correlate to the intensity of the atomic concentration in the sample.[8]

Inductively coupled mass spectrometry (ICPMS) introduces the sample as solution or fine particles entrained in a gas flow. Drying and ionizing of the sample occurs in an Ar plasma, rather than on a filament as done in TIMS. The sample solution is fed through fine tubing into a nebulizer and is subsequently aspirated into the Ar plasma channel. The high temperature of the plasma first dries the aerosol droplets, atomizes the dried sample, and finally ionizes the resulting atoms. The cations are then focused and accelerated through the mass separation components. While some systems use electromagnets to spatially separate the beam, the majority of ICPMS systems use quadrupole mass analyzers. In the quadrupole, the ions are exposed to a varying electric field. The frequency and intensity of the electric field can be set such that ions without the desired mass to charge ratio will attain degenerate trajectories leaving only the desired

ions to transmit through for detection. Detection is accomplished similarly to TIMS, using FCs or electron multiplier detectors. [9]

Accelerator mass spectrometry (AMS) sample introduction methods involve the sputtering by cations, most commonly Cs^+, of a solid sample target in order to atomize the sample and generate anions of the desired analyte. This is accomplished by feeding Cs gas into the source vacuum where it becomes thermally ionized by collisions with a heated (1200^o C) spherical tungsten electrode. The cations are focused onto the target which acts as a cathode. As the sample becomes atomized, the anions that are generated will be accelerated out of the source. The components used in mass filtration include: electrostatic analyzers (ESA) (which separate the beam according to ion energy), electromagnets, and a tandem accelerator. The tandem accelerator accelerates the anion beam, strips the ions of electrons, and reaccelerates the cation beam up to very high energies. The electron stripping also breaks apart most molecular interferences. Thus, the accelerator enables the measurement of very low concentration samples where the spectrum would normally be dominated by neighbouring mass interferences. Detection and quantification of the beam is accomplished through the use of Faraday cups, which handle large beam currents, and gas ionization chamber (GIC) detectors, for single atom counting where beam currents are too small to be measured by Faraday cups. [10, 11]

The following section outlines the physical principles behind the anion beam generation, mass filtration (such as the ESA and electromagnet), and ion detection techniques used in AMS.

1.3 Principles of Accelerator Mass Spectrometry

Mass spectrometry analyzes a sample by ionizing the atoms then, using the Lorentz force (Eq. 1.1), separates them according to their mass.

$$\vec{F} = q(\vec{E} + \vec{v} \times \vec{B}) \tag{1.1}$$

This is accomplished by, first, adding an overall charge to the atom. To produce negative ions, the sample target is sputtered with an energetic ion, most commonly Cs^+ as it is a good electron donor, that releases and ionizes the surface atoms. The ion source used for this research can be seen in figure 1.1 with a more detailed diagram in figure 1.2.

Once a sample atom has been ionized, the ions of charge state (q) are focused and accelerated through a voltage potential (V) giving them an initial kinetic energy (K). This exchange in energy can be represented as a conservation of energy equation:

$$\begin{aligned} \Delta U_e + \Delta K &= 0 \\ q\Delta V + \frac{1}{2}m(v_2 - \cancelto{0}{v_1})^2 &= 0 \\ \frac{1}{2}mv_2^2 &= -q\Delta V \end{aligned} \tag{1.2}$$

where U_e is the electric potential as determined by the source, m is the ion mass and v is the ion velocity. As can be seen from equation 1.2, all ions leaving the source that have the same charge state, have the same energy, but different momentum depending on their mass. Each ion will have some fraction of their energy in the radial direction. Therefore, to ensure the ions remain on the beam line axis, various electrostatic lenses

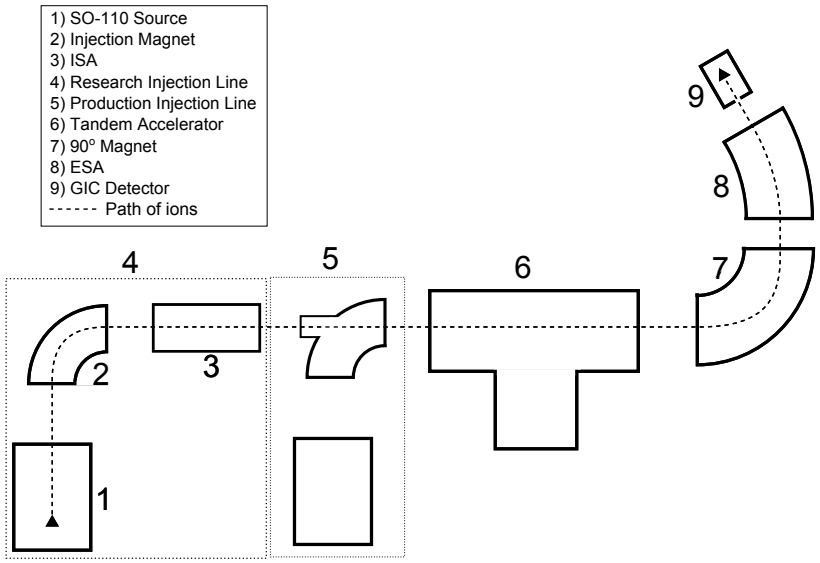

Figure 1.1: Diagram of the IsoTrace AMS system as viewed from above.

are used in between analyzing components.

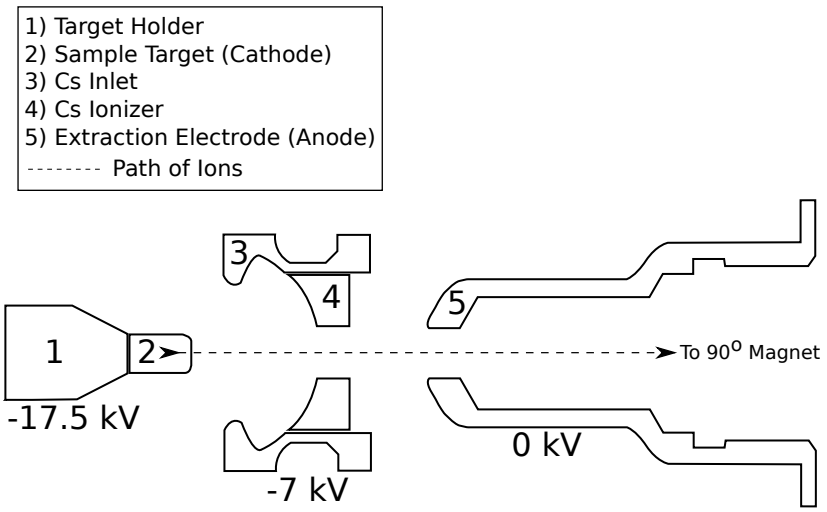

Figure 1.2: Cross sectional diagram of the SO-110 Sputter Source.

The next step is to make the initial separation by mass. This is done using a curved electromagnet. The ray of ions enters the magnet where they are exposed to a magnetic field (B). The magnetic field applies a perpendicular force (F_B) to the beam of ions which causes it to follow a curved trajectory of radius (r). Equation 1.3 demonstrates how the magnet selects the desired mass to analyze.

$$\begin{aligned} \vec{F}_B &= q\vec{v} \times \vec{B} \\ m\frac{v^2}{r} &= qvB \\ \frac{\frac{1}{2}mv^2}{\frac{1}{2}q}\frac{m}{q} &= (rB)^2 \\ \frac{K}{q}\frac{m}{q} &= \frac{(rB)^2}{2} \\ B &= \frac{\sqrt{2Km}}{rq} \end{aligned} \tag{1.3}$$

Since all the ions have the same kinetic energy, letting r be the magnet's radius of curvature, q the overall charge of the ion, and m the mass of the ion we want to measure, the magnetic field can be found. At this field, the mass of interest will follow the curvature of the magnet while heavier masses will curve less and lighter masses will

curve more.

This simple form of a mass spectrometer produces a rudimentary mass spectrum. This spectrum, however, is often insufficient for determining the specific atoms that make up the beam due to interferences from: isobars (molecules or isotopes of different atoms with the same mass), tailing from neighbouring masses (due to energy spread of the abundant isotope), and atoms or molecules with equal mass to charge ratios. Therefore, additional separation techniques are required.

In accelerator mass spectrometry, following the bending magnet phase, the ion beam is sent into a tandem accelerator. Here the anions that were generated in the source are accelerated to the center of the tandem through a large electric potential. The anion beam loses electrons to the electron stripper, gaining an overall positive charge, and is then reaccelerated as cations, utilizing the same electric potential to accelerate the beam out of the tandem. The purpose of the tandem is twofold: it removes molecular interferences through collisional dissociation in the stripper gas, and facilitates the detection of the ions by high energy particle detectors, such as a GIC detector. The energy of the ions after acceleration is defined by equation 1.4.

$$K_{\text{total}} = q_1 \frac{m}{M}(V_{\text{source}} + V_{\text{tandem}}) + q_2 V_{\text{tandem}} \tag{1.4}$$

Where M is the mass and q_1 is the charge of the initially accelerated atom or molecule. Likewise, m and q_2 are the mass and charge of the analyte ion after charge exchange occurs in the stripping canal of the tandem. The term $\frac{m}{M}$ is required here for the case when the isotope of interest is initially accelerated as a molecule. When this molecule is dissociated in the tandem, the kinetic energy is apportioned, leaving the atom with its fraction of the initial energy.

Following the tandem, another magnet bends the high energy beam. However, due to the increase in kinetic energy, the magnetic field must have a higher magnitude to bend the beam (Eq. 1.3).

At this stage, however, the combination of sputtering, molecular fragmentation, and collisional scattering of the ions results in an energy spectrum with poorly defined peaks. The large tails of the energy spectrum can severely limit the resolution of neighbouring masses. The tailing of the spectrum can be improved with the use of an electrostatic analyzer (ESA) which manipulates the cation beam using an electric field (E) much like a bending magnet does with a magnetic field. The beam separates in the ESA according to:

$$\begin{aligned} \vec{F}_E &= q\vec{E} \\ m\frac{v^2}{r} &= qE \\ \frac{K}{q} &= \frac{rE}{2} \\ E &= \frac{2K}{rq} \end{aligned} \tag{1.5}$$

By using the K_{total} calculated for the atom of interest the desired E for the ESA can be determined. An ESA can also be used at the low energy end before the injection magnet to remove the tailing from the sputter source before acceleration.

Finally, the beam must be collected in a detector for quantification. This is often a GIC detector. The only remaining particles in this beam should theoretically be the atoms of interest as well as any atoms that exhibit equal mass to charge ratios. It is the role of the detector to differentiate among these remaining atoms. Due to the difference in proton number, the atoms will lose their remaining energy at different rates within the isobutane gas. By measuring the amount of energy lost within the detector, the atoms can be identified. The GIC detector is one of the key elements which allows an AMS system to measure very low abundance samples as the background interference in the region of interest is effectively zero counts. A diagram of the AMS system used in the following experiments can be seen in figure 1.1.

1.4 Purpose

The purpose of these experiments was to: demonstrate the removal of interferences from a Cs anion beam, develop measurement techniques to produce the first measurements of rare Cs isotopes by AMS, and apply these techniques to make a measurement of the half life of ^{135}Cs.

Chapter 2

Background

2.1 Techniques for Measuring Long Lived Caesium Radioisotopes

Techniques for the detection and quantification of radioisotopes in a sample can be divided into two types. The first approach involves the detection of decay products from the sample. As a radioisotope decays it emits characteristic radiation that can be detected through spectroscopic methods. The decay scheme for ^{135}Cs and ^{137}Cs can be seen in equation 2.1. Depending on the kind of radiation emitted, this can be alpha, beta, or gamma spectroscopy. This type of detection is most efficient for samples with short half lives that decay quickly, emitting their characteristic products frequently. However, this method of isotope detection is impractical for the detection of long-lived (>1Ma) isotopes and cannot be used for stable isotopes, whereas the second technique excels in these respects. This method involves separating the isotopes by their mass and counting the number of ions of the mass(es) of interest individually. This can be done in several ways, each with their own advantages and disadvantages.

$$
\begin{aligned}
^{135}Cs &\xrightarrow{\beta^- decay} {}^{135}Ba + \beta^- + \nu \qquad (t_{1/2} = 2.3Ma) \\
^{137}Cs &\xrightarrow{\beta^- decay} {}^{137m}Ba + \beta^- + \nu \qquad (t_{1/2} = 30.17a)
\end{aligned}
\tag{2.1}
$$

While there are many variants, mass spectrometry for radionuclides can be divided into three general forms: thermal ionization mass spectrometry (TIMS), inductively coupled mass spectrometry (ICPMS), and accelerator mass spectrometry (AMS).

TIMS techniques for Cs isotopes have been reviewed by Lee et al. TIMS is generally considered to be a more precise technique than AMS and ICPMS and is frequently used for isotope ratio measurements. With respect to the long-lived Cs isotopes, TIMS has been shown to measure ^{135}Cs precisely in samples containing abundance ratios of $^{135}\text{Cs}/^{133}\text{Cs} = 10^{-9}$.[1] However, this technique requires a large time investment in the sample preparation to ensure analyte purity.

ICPMS is another mass spectrometry technique. It's applicability to radioisotope measurement was reviewed by Lariviere et al. ICPMS doesn't require as exhaustive sample preparation procedures as those needed for TIMS and has been shown to be able to measure samples which contain fg levels of Cs (10 fg mL^{-1} of ^{135}Cs and 6 fg mL^{-1} ^{137}Cs) by utilizing an on-line reaction cell to minimize isobaric interferences. Furthermore, this process has allowed ICPMS to measure ^{135}Cs at an abundance sensitivity of 1.3×10^{-9}. [2, 12]

AMS is the third mass spectrometry approach used for radioisotope measurement and was recently reviewed by Litherland et al and Hellborg and Skog. AMS consistently reports faster sample turn around times and has abundance sensitivity reaching as low as 10^{-18}. This technique had yet to be used to measure radioactive isotopes of Cs. The detection limit of AMS for radioactive Cs isotopes, just as it is with other forms of mass spectrometry, is limited by interferences from atomic isobars, among other things. [10, 11]

2.2 Accelerator Mass Spectrometry and Isobaric Interferences

Accelerator mass spectrometry is most commonly used for the measurement of radiocarbon for the purpose of carbon dating.[13] This is due to the ability of AMS to remove the abundant ^{14}N from the desired ^{14}C signal. As the electron affinity of the N atom is negative, N does not form a negative ion while the C is ionized to produce the C^- beam. Additionally, due to high particle energy after the tandem accelerator, the interference from the large abundance difference between ^{14}C and ^{12}C is minimal.

Often, however, the electron affinity of the interfering isobar is positive, complicating the isobaric elimination. In the case of Cs, the Ba interference can be attenuated by analyzing the ions in molecular fluoride form, CsF_2^-. Since Ba preferentially forms BaF_3^-, there is an immediate suppression of >99% of Ba interference.[14] This is often not a sufficient suppression. Therefore, additional processes are required.

To date, the method of isobar separation has involved lengthy column chemistry procedures. The Cs samples are mixed with a Cs specific resin, ammonium 12-molybdophosphate (AMP), which binds the Cs atoms in a Cs-AMP complex. This resin can then be dissolved afterwards to release the Cs for analysis. This process has been used in a wide range of nuclide detection techniques either to remove isobaric, ^{137}Ba, or radioactive, ^{87}Rb, interferences.[1, 15, 16] This process alone however, is not capable of eliminating the ubiquitous Ba contamination to the levels that are needed for any measurement of ^{135}Cs in environmental samples.[12] This, and similar requirements have led to the development of more advanced techniques for the elimination of isobars in MS.

Recently, the on-line removal of isobaric interferences has been accomplished with collision or reaction cells, incorporating radiofrequency quadrupole ICPMS for many isobar/analyte systems, including ^{135}Cs and ^{135}Ba.[16] In conjunction with the AMP chemistry mentioned previously, these procedures have reported sensitivities as low as

10 fg/ml for ^{135}Cs with a Ba attenuation of 10^4.[17] With the success of on line isobaric attenuation mechanisms for ICMPS, a similar device, the Isobar Separator for Anions (ISA) was constructed to test for similar results using AMS.[18]

2.3 Isobar Separator for Anions

The basic functions of the ISA [19] are to:

- Accept the beam of anions coming from the injection magnet.
- Decelerate the beam.
- Capture the beam in a radiofrequency field.
- React the beam with a gas.
- Reaccelerate the beam into the rest of the AMS system.

The ISA for AMS has shown a lot of promise since its inception, demonstrating the ability to suppress the isobars of wide range of isotopes (e.g. ^{41}Ca, ^{36}Cl, ^{90}Sr,^{182}Hf, and ^{135}Cs). [4, 20] In the case of ^{135}Cs, the ISA has been shown to suppress the isobaric ^{135}Ba signal by a factor of 2×10^{-5} using NO_2 reaction gas, attenuating the signal 20 times more than the on-line suppression reported for ICPMS.[17] Tests on Cs however, have only characterized the ISA in terms of its suppression and transmission. Actual isotopic analyses have yet to be completed using the ISA.

2.4 Determining Half-Lives of Nuclides

An accurate measurement of an isotopes half life is required if it is to be used for radiometric dating or to compare mass spectrometry and nuclear decay measurements. To measure half life, two values are needed: the amount of radioisotope in a sample and the decay rate of that sample. The half life of ^{137}Cs was determined by gamma decay counting a standard amount for over a decade, finding the half life to be $30.17 \pm 18\%$

years. [21] Currently, there are two measurements of the ^{135}Cs half life, each reporting large uncertainties in the values. Due to the difficulty of obtaining and measuring ^{135}Cs directly, these experiments measured a known amount of ^{135}Xe and allowed it to decay into ^{135}Cs which was then beta counted to determine the activity.[22, 23] With the advent of isobar separation in mass spectrometry, the ability to measure ^{135}Cs directly is now possible, allowing for a potentially more accurate measurement of its half life.

The half life of ^{135}Cs must be determined if it is to be used to supplement the well established ^{137}Cs radiometric dating applications.[1] Previously, an effective technique for measuring the half life of a long lived isotope, ^{41}Ca, involved measuring the activity by liquid scintillation counting (LSC) and determining the analyte composition using TIMS.[24] Therefore, by utilizing this technique with ^{135}Cs and the ISA-AMS system, this thesis reports a new measurement of the half life of ^{135}Cs.

Chapter 3

Barium Suppression and Development of Measurement Techniques

This chapter has been accepted for publication in Rapid Communications in Mass Spectrometry.

3.1 Introduction

The usefulness of ^{134}Cs and ^{137}Cs as analytical tools has been well established in radiation protection, age dating, environmental analysis, and nuclear forensics.[25, 26, 16, 27] Some of these applications rely completely on the ^{137}Cs that was created in atmospheric nuclear weapons testing in the mid 20th century which effectively spiked the planet with fission product isotopes that would not occur otherwise. ^{134}Cs and ^{137}Cs, however, have relatively short half lives (2.3a and 30a respectively) which means that the amount of ^{137}Cs that was created during weapons testing has undergone a few half lives already, making it increasingly difficult to measure. ^{134}Cs is not created in weapons fallout and any released into the environment from the Chernobyl reactor accident has all decayed.

In 2011, the Fukushima incident released a large amount of ^{134}Cs, however this will all decay away soon. ^{135}Cs is created with nearly the same fission yield as ^{137}Cs (6-7%) and has a half life of 2.95 Ma[23] making it a possible candidate for long term analysis. With such a long half life, traditional methods of decay measurement become impractical promoting the development of measurement by mass spectrometry. TIMS and ICPMS have been used to measure ^{135}Cs.[28, 16, 1] We are therefore motivated to develop AMS for the measurement of Cs isotopes.

The current detection of Cs by AMS (^{135}Cs/^{133}Cs 5×10^{-7})[29] is about 10^5 times higher than levels in the environment from weapons test fall out and the detection limit is determined by isobaric interferences, Ba being the most prominent. The Isobar Separator for Anions has proven quite effective at on-line removal of isobars (e.g. ^{41}Ca, ^{36}Cl, ^{90}Sr,^{182}Hf, and ^{135}Cs)[4, 20]. The purpose of this report is to describe the first detection of ^{135}Cs by AMS at the IsoTrace Laboratory, University of Ottawa.

3.2 Methods

The largest challenge for measuring Cs isotopes by AMS is the isobar interference from Ba. Although Ba contamination can be greatly reduced by sample preparation techniques, it is still insufficient when it comes to the detection of rare long-lived ^{135}Cs at its natural levels. [28, 15] Previous ISA configurations have proved effective at eliminating Ba from a CsF_2^- ion beam using NO_2 reaction gas; however the transmission of the Cs analyte was also poor.[4] In these experiments, O_2 was used in the gas cell in an attempt to reduce potentially severe losses of CsF_2^- by adduct formations with the radical species NO_2.

It is difficult to make Cs anions due to its valence electron structure, so it is necessary to accelerate it as a molecular ion, CsF_2^-. To accomplish this, the samples used in these experiments were prepared as follows. PbF_2 (Alfa Aesar Puratronic 99.999%) was added

into pre-weighed clean 15 mL round-bottom Savillex PFA vials. Known amounts of ^{134}Cs, ^{135}Cs and Ba solutions were drawn into PTFE micro-tubing and weighed on a precision Mettler-Toledo microbalance before being expelled into the Savillex vials. 20 drops of 28.9 M HF were then added from a clean PFA Teflon dropper bottle directly into the Savillex vials containing the PbF_2 + Cs or Ba. The mixture was capped tightly and fluxed inside an isolated, vented plexiglass box at 90^{o}C on a hotplate in their same Savillex capsules with occasional swirling for at least 2 hrs. Samples were slowly evaporated to dryness for >5 hrs on the same hotplate at 90^{o}C by removing the lids of the Savillex capsules; HF fumes were withdrawn under mild suction from inside the plexiglass. The final samples consisted of a dry material that were then loaded into 1.3 mm diameter stainless steel target pieces and pressed under 0.6 GPa of pressure.

While ^{134}Cs and ^{137}Cs can be purchased as standards, the ^{135}Cs contamination in them is not quantified. Therefore, the samples of pure ^{134}Cs and ^{135}Cs had to be produced. The ^{134}Cs was made through the neutron activation of $^{133}Cs_2CO_3$ at the Royal Military College of Canada Slowpoke reactor and the ^{135}Cs was supplied by Chalk River Laboratories via a section of pipe from their Xe isotope production facility. This pipe was washed with distilled water to collect the Cs that had been deposited there by Xe decay. Through beta and gamma spectroscopy, the wash was shown to contain only ^{135}Cs with minimal ^{137}Cs contamination.

The isobaric attenuation in this experiment utilized the stability of Cs in its superhalogen form. When the anions were produced in the source, Ba preferentially forms BaF_3^- (the formation ratio of BaF_2^- to BaF_3^- is <1%) while Cs preferentially forms CsF_2^- (>99% compared to other CsF_n^- molecules).[14] Therefore, by selecting this anion, there is an immediate elimination of >99% of the Ba contamination. This phenomena was further exploited in the gas cell where BaF_2^- has a greater chance of reaction compared to the more stable CsF_2^- superhalogen.

In order to maximize the efficiency of Cs transmission while still eliminating the Ba

background, an attenuation profile was created. This was accomplished by measuring the transmission of ^{133}Cs and ^{136}Ba at increasing gas cell pressures using PbF_2+^{133}Cs and PbF_2+Ba targets . The ISA-AMS system was tuned using a $^{133}CsF_2^- \rightarrow {}^{133}Cs^{+3}$ pilot beam for gas cell pressures ranging from 0 to 0.8 Pa of O_2. The system tuning for each pressure was recorded and reapplied for the $^{136}BaF_2^- \rightarrow {}^{136}Ba^{+3}$ transmission measurement. A comparison of the relative transmissions can be seen in figure 3.1.

The ISA was tested for mass dependent bias. Ba is an ideal surrogate for Cs for this test as all operating parameters are identical to measuring Cs, specifically: masses of interest, initially accelerated molecule, and charge state after the accelerator electron stripping canal. The results were compared with the known natural abundance of Ba isotopes.

The measurement of an unknown amount of ^{135}Cs by AMS was demonstrated using ^{134}Cs as a yield tracer. The ISA-AMS system was tuned using the ^{133}Cs pilot beam at 0.53 Pa of O_2 in the ISA gas cell. Ions of ^{134}Cs and ^{135}Cs were accelerated as $CsF_2^- \rightarrow Cs^{+3}$ and measured in the final gas ionization chamber (GIC). ^{136}Ba (7.9% natural abundance) was measured periodically throughout analysis to ensure that there was no Ba contamination in the 134 (2.4% natural abundance) and 135 (6.6% natural abundance) mass spectra.

3.3 Results and Discussion

Figure 3.1 demonstrates the effectiveness of O_2 for the attenuation of Ba. The operating pressure of 0.53 Pa was able to attenuate the Ba beam by a factor of 2×10^5 while 25% of Cs was transmitted through the ISA.

Relative to the NO_2 attenuation, the O_2 in the ISA had greater attenuation of Cs and poorer attenuation of Ba. At higher pressures, however, the CsF_2^- transmission starts being suppressed in NO_2 while CsF_2^- transmission in O_2 plateaus. Therefore, NO_2 reduces the BaF_2^- beam more effectively than O_2 at lower pressures while at higher

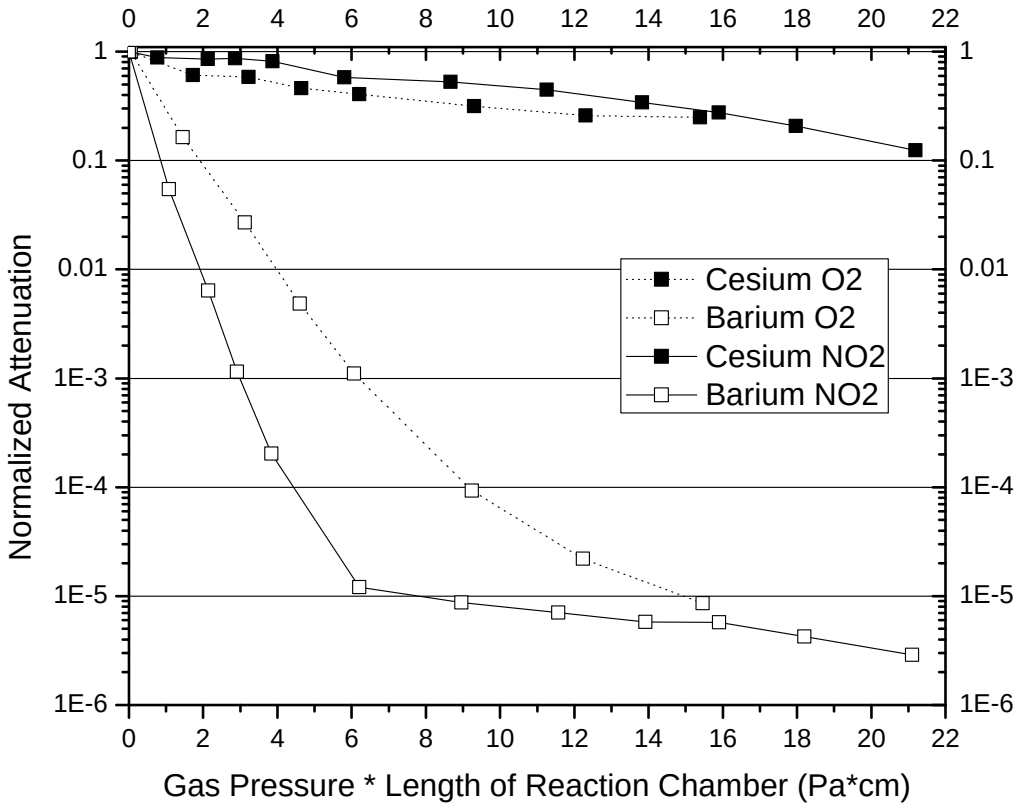

Figure 3.1: Normalized attenuation curves of Cs and Ba in O_2 and NO_2. Due to the different configurations of the ISA gas cell (15cm long for NO_2 [4] vs. 23cm long for O_2 [5]) the attenuation curve is represented as attenuation per cm of gas cell per Pa of O_2 pressure.

pressures, >16 Pa·cm, the transmissions are similar. Further experimentation could be done in order to better understand the mechanism of suppression by analyzing the attenuated beam for $BaF_2^- + NO_2/O_2$ reaction products, electron detachment products, and molecular destruction products.

The ability of the ISA-AMS to maintain consistent efficiency for each isotope is demonstrated in figure 3.2. Here, the measured abundance of Ba isotopes (134, 135, 137, and 138) in the sample is compared to the known natural abundance. The ISA-AMS system performed well, producing a slope of 0.991±0.0083 (R^2=0.9997). Therefore, there does not appear to be any significant mass dependent bias (at the level of ±0.8%)

in the sample preparation, isobar separation, or measurement phases of the experiment. Additional experiments are needed to test for mass fractionation at the per mil level.

The process of isotope dilution or yield tracing is a powerful tool in radioanalytics used to account for losses in analyte during the sample preparation and measurement process. In order to analyze ^{135}Cs, ^{134}Cs can be used as a yield tracer because it can be produced with negligible ^{135}Cs contamination. The results from the Ba isotope measurements support the use of yield tracing for measuring Cs isotopes by ISA-AMS.

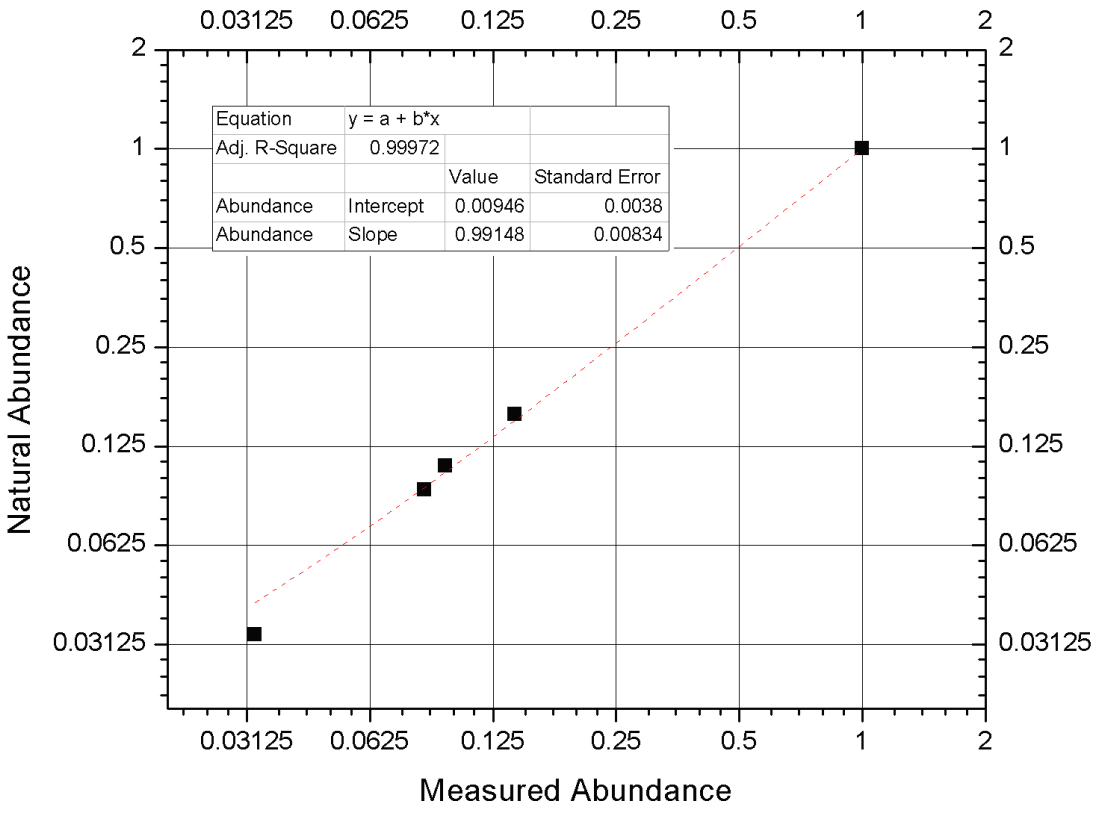

Figure 3.2: Comparison of measured abundance of Ba isotopes in sample targets to the known natural abundance. The dotted red line represents the linear fit of the data, having a slope of 0.991 ± 0.0083. The uncertainty in counting statistics is smaller than the symbols in the figure.

Normally, when analyzing a sample by AMS, the rare and abundant isotopes are measured concurrently in different detectors. This practice, however, was not possible

as the sputter source uses $^{133}Cs^{+}$ (the abundant isotope) to sputter the samples. In this instance, the ISA-AMS system had to be sequentially tuned for each isotope to be measured in the final detector as fast isotope switching was not possible on the ISA injection line at IsoTrace. In the future, a different anion, such as rubidium, could be used to sputter the samples.

Figure 3.3 shows a typical spectrum for Cs analysis. The GIC is able to separate cations that have equal mass to charge ratios, this proved very important for measuring $^{135}Cs^{+3}$ due to interferences from $^{45}Sc^{+1}$ and $^{90}Zr^{+2}$. Although these cations can produce large signals (e.g. $^{45}Sc^{+1}$ in figure 3.3) the separation is large enough that there was no interference from tailing.

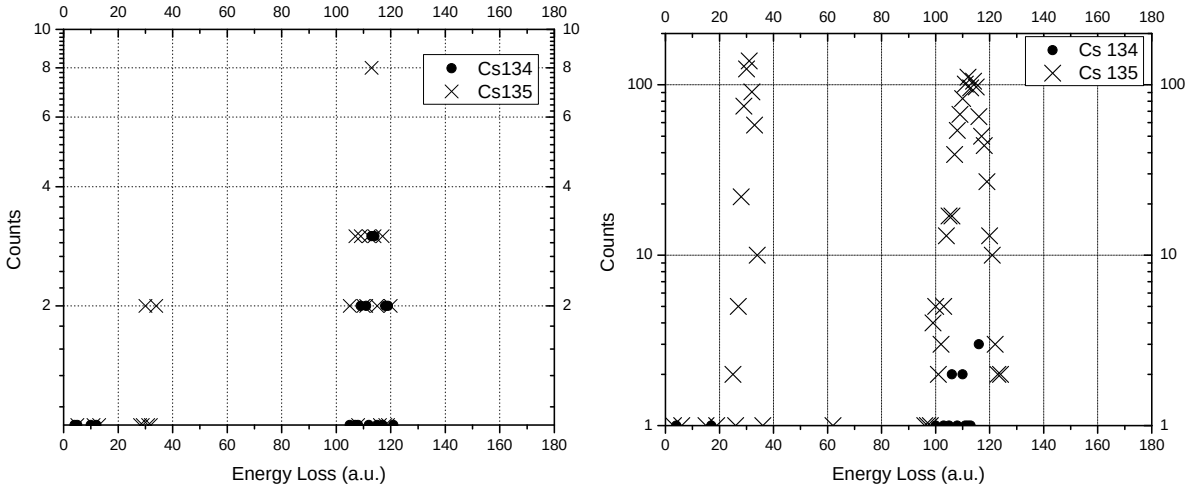

(a) Target 1 (b) Target 2

Figure 3.3: The GIC spectrum of ^{134}Cs and ^{135}Cs with 0.53 Pa of O_2 in the gas cell. These samples contain approximately 1.8×10^{12} atoms of ^{134}Cs and 5.3×10^{13} atoms of ^{135}Cs. The $^{45}Sc^{+1}$ peak is located at 30 au.

All measurements made on the ISA with 0.53 Pa of O_2 had 0 counts of mass 136 in 20 minutes. By extension it can be concluded that there was no Ba interference in the mass range of interest as ^{134}Ba and ^{135}Ba are less abundant than ^{136}Ba. Had there been 1 count of Ba in the 20 minute analysis period this would correspond to a detection limit of 5×10^{10} atoms per target. No counts were obtained at mass 137 which was expected as the amount of ^{137}Cs present (5×10^{6} atoms per target) was below detection limits.

Currently, work is being done to further develop this analytical technique by increasing Cs current and decreasing the detection limit. Since Cs preferentially forms a cation the use of cation injection single stage AMS should be explored.

3.4 Conclusion

The ISA suppressed the Ba isotope interference by 5 orders of magnitude while transmitting 25% of the original Cs beam. The Ba beam was suppressed by NO_2 and O_2 in similar amounts. There was no fractionation of Ba isotopes (at the 0.8% level) using this ISA-AMS procedure. Further experimentation is still required to increase efficiency of the Cs in ISA-AMS in order to measure samples containing naturally abundant Cs. The use of ISA-AMS for ^{135}Cs analyses in environmental studies is very promising.

Chapter 4

Measurement of Caesium by AMS

In order for a technique such as ISA-AMS to be relevant as a routine analytical method its operating parameters must be optimized and its sample requirements and limitations must be determined. These latter data provide a baseline for experimenters to evaluate the technique and to determine whether the technique is suitable for their purposes. In order to analyze Cs isotopes by AMS, a Cs anion beam must be produced in the ion source with a high enough efficiency to minimize the use of valuable sample material and analysis time. Many factors can affect the efficiency of an isotope. These include:

1. Ionization efficiency: The production of the desired ion by the ion source.

2. Isobar suppressor efficiency: The transmission of analyte through the on-line separation of isobars.

3. System efficiency: The transmission of the ion beam through mass filters, electron stripping canal, and other system components.

The purpose of this chapter is to examine these factors to determine the best operating conditions and the limitations.

4.1 Experimental Approach

These experiments were done at IsoTrace Laboratory, the accelerator mass spectrometry facility operated by the University of Ottawa.

After sample preparation and target creation (described in chapter 3.2), the targets were loaded into an SO-110 sputter source (High Voltage Engineering B.V., the Netherlands) for analysis. Due to the relatively large mass of the molecular anion being accelerated (m[CsF_2] = 171 amu) the initial extraction voltages were kept low to permit the analysis of the beam by the injection magnet, the field of which could not exceed 0.5 T. The SO-110 operating parameters for these experiments can be seen in table 4.1.

Table 4.1: SO-110 operation parameters for Cs measurements.

Parameter	Value
Target Voltage	-7 kV
Extraction Voltage	-10.5 kV
Cs Boiler	90 ^{o}C
Ionizer Current	17 A

Following the source, the beam goes through a low energy injection magnet, isobar separator for anions, tandem accelerator, high energy bending magnet, electrostatic analyzer, and finally gas ionization chamber detector. Due to the inability of the system to switch automatically between desired ion beams, the system had to be manually tuned for each mass. The operating parameters are listed in table 4.2.

Table 4.2: Operating parameters for sequential measurements. B1 and B2 are the fields of the injection and high energy magnets.

Isotope	Mass 1 (amu)	B1 (T)	Terminal (MV)	Mass 2 (amu)	B2 (T)
Cs133	170.9022534	0.43390	1.3505	132.90544	0.98656500
Cs134	171.9035064	0.43514	1.3500	133.90670	0.99026279
Cs135	172.9026964	0.43642	1.3496	134.90589	0.99397331
Ba136	173.9013764	0.43770	1.3491	135.90456	0.99762948
Cs137	174.9038764	0.43900	1.3487	136.90707	1.00132165

Using these procedures, Cs was measured on an ISA-AMS to perform the first assessments of the behaviour of radioactive Cs beams and the efficiencies and limitations

of different approaches for analysis.

4.2 Caesium Beam Current and Efficiency

Cs does not produce an atomic negative ion due to its valence electron structure; this effect immediately diminishes the efficiency of Cs measurement by AMS unless an intense molecular beam can be obtained from the ion source. Initial tests to determine the optimal operating parameters for Cs were done using targets that had high concentrations of CsF in the PbF_2 matrix, each target containing approximately $(0.5 - 2) \times 10^{19}$ atoms of ^{133}Cs. Due to the hygroscopic nature of CsF, targets were only created up to a concentration of 30% CsF to PbF_2 by mass. Concentrations higher than this quickly absorbed environmental moisture, compromising the integrity of the sample. Typical Cs currents measured at the Faraday cup located just after the injection magnet can be seen in figure 4.1. It was found that lower concentrations of CsF, 7% by mass, produced around 75 nA. Additionally, mixing the samples by fluxing (as described in section 3.2) in HF produced more stable currents due to the better homogenization of the material.

During experimentation with Cs radioisotopes, however, samples were produced at much lower Cs concentrations. Targets composed of ^{134}Cs and/or ^{135}Cs contained approximately 2×10^{12} and 5.5×10^{13} atoms respectively, a factor of $\sim 10^6$ times less than stable Cs samples. Sample compositions for these tests can be seen in table 4.3. Mass 134 and 135 measurements were taken at the final GIC detector. Here, count rates of 0.3 ± 0.2 cps and 4 ± 3 cps for ^{134}Cs and ^{135}Cs were recorded. All reported currents were normalized to 1 nA of ^{133}Cs current.

Table 4.3: Samples used in the Cs radioisotope experiments.

Sample	PbF_2 (mg)	^{134}Cs atoms	^{135}Cs atoms
Blank	46.1	0	0
^{134}Cs	32.3	1.9×10^{12}	0
^{135}Cs	33.2	0	5.4×10^{13}
$^{134/135}$Cs	33.9	1.8×10^{12}	5.6×10^{13}

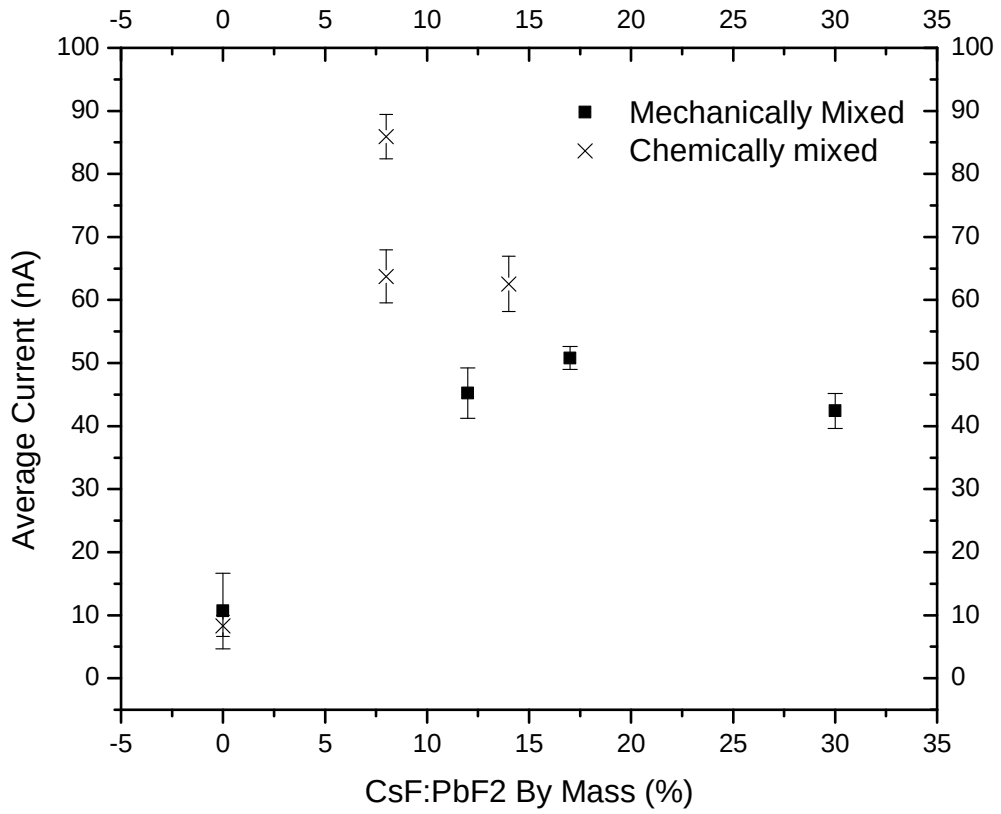

Figure 4.1: Average ^{133}Cs currents over 20 minutes measured after the injection magnet. Samples marked with (•) were mixed using a stir rod and the samples marked with (×) were mixed by fluxing with HF. Error bars represent the stability of the beam over the 20 minute analysis period.

Table 4.4: The measured efficiencies of the AMS system components.

Component	Efficiency
ISA @ 0.53 Pa of O_2	25%
2nd Injection Magnet Box	57%
Tandem	45%
HE Magnet + ESA	26%
Total	**1.7%**

Two factors limit the detection of Cs: the transmission efficiency of the AMS system and the ionization efficiency of Cs. The efficiency of the components of the Isotrace Laboratory AMS system can be seen in table 4.4. The magnet box listed in this table is the section of beam line between the ISA and the tandem that is occupied by the injection magnet of the production injection line. Ionization of Cs and formation of CsF_2^- has a

much larger impact on efficiency. The low concentration radio-caesium targets produced a total measurement efficiency of 1.7×10^{-9} which, accounting for AMS efficiencies, results in an ionization efficiency of 10^{-7}. It should be noted however, that these efficiencies are based on the sequential measurement method outlined in section 3.3. This process results in only 25% of the target measurement time being spent on a particular isotope.

4.3 Interferences and Crosstalk

All isobaric interferences need to be eliminated in order to measure a concentration of ^{135}Cs. The Isobar Separator for Anions (ISA) described in section 2.3 was used to suppress the isobaric interferences from $^{134/135}$Ba. It was found that 0.53 Pa of O_2 gas in the reaction cell of the ISA was sufficient for the removal of Ba while maintaining a usable Cs signal.

In addition to Ba, there was an unanticipated interference from Zn dimers which span the mass range of interest (figure 4.2). The mechanism of interference can be seen in table 4.5. These molecular interferences were eliminated by increasing the stripper pressure in the tandem accelerator until no counts were seen in mass 136. It was found that all dimer interferences were suppressed at a stripper gas pressure which resulted in a pressure of 2.1×10^{-7} mBar at the low and high energy ends of the tandem accelerator. This corresponds to a stripper gas thickness of $0.5\mu g/cm^2$.

Source memory effects introduce crosstalk between samples inside the source. This occurs when a target ejects some material into the source environment, contaminating subsequent target measurements. This process was observed in the Cs measurements (figure 4.3).

During analysis, a large emission of target material was observed after a few minutes of sputtering as indicated by a drop in target voltage, due to the emission of ions and electrons, and a spike in target current, caused by the source attempting to maintain

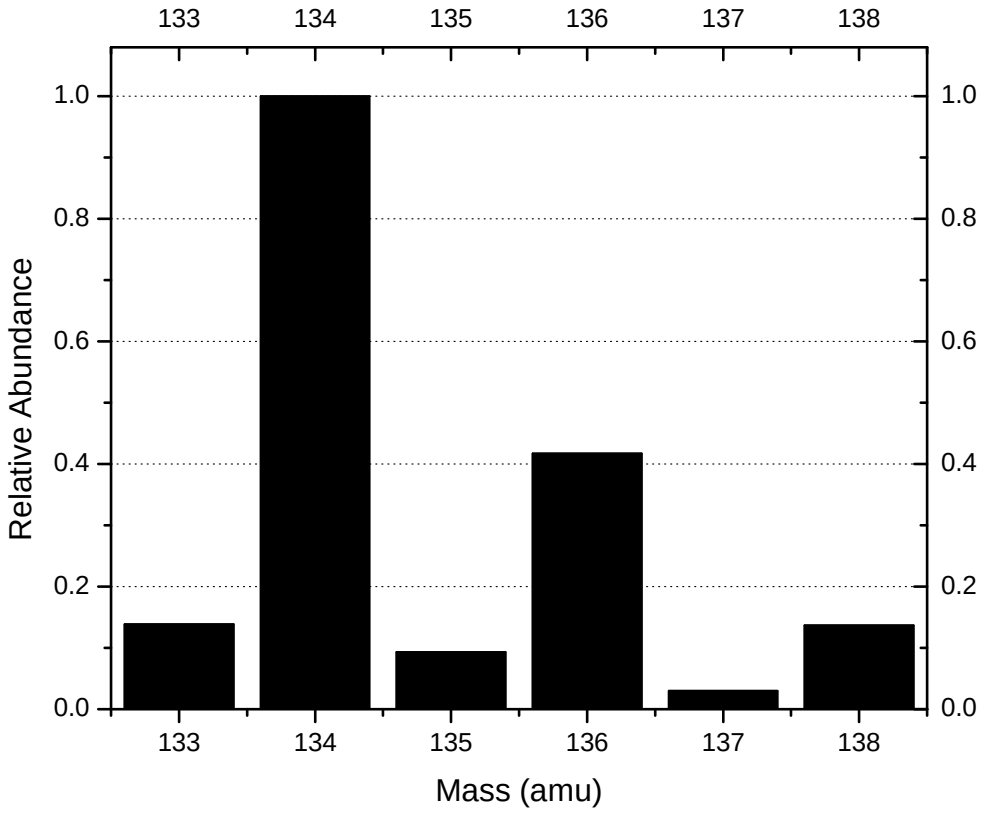

Figure 4.2: Abundance of the interfering Zn dimers that can interfere with Cs isotope measurements. The dimer abundance is calculated by determining the probability that any two Zn isotopes will add to a given mass. These probabilities were then normalized to the most abundant Zn dimer, mass 134. For example, a dimer of mass 136 can be a combination of Zn isotopes of mass 66 (28% abundance) and 70 (6% abundance) or 68 and 68 (19% abundance).

voltage. It is hypothesized that this event is due to the inefficient removal of heat from the sputtered surface, causing instability in the target material. Any un-ionized Cs ejected from the target during this emission event creates a partial pressure of sample Cs in the source. This partial pressure remains in the source during the analysis of subsequent targets. Cross contamination occurs when previously ejected Cs from the source environment becomes ionized by the source ionizer. The ion optics of the source, which are designed for Cs^+, focus the ionized Cs to the target surface, allowing it to be reemitted and accelerated through the machine.

Table 4.5: Comparison of Cs and Zn energy and mass characteristics as they would be analyzed by different AMS mass filters. A source voltage of -17.5 kV and tandem accelerator voltage of 1.3496 MV was used for these calculations. Values expressed in units of elementary charge, MeV, and atomic mass units. The initially accelerated molecule of Zn was not directly measured, therefore the molecule is represented as $Zn_2[38]^-$.

	Cs 135			Zn Dimer		
AMS Component	Form	mE/q^2	E/q	Form	mE/q^2	E/q
Source	CsF_2^-	3.026	0.01750	$Zn_2[38]^-$	3.025	0.01750
Injection Magnet	CsF_2^-	3.026	0.01750	$Zn_2[38]^-$	3.025	0.01750
Tandem (Mid)	Cs^{+3}	143.900	1.06667	Zn_2^{+3}	143.827	1.06655
Tandem (End)	Cs^{+3}	76.679	1.70282	Zn_2^{+3}	76.646	1.70278
HE Magnet	Cs^{+3}	76.679	1.70282	Zn_2^{+3}	76.646	1.70278
ESA	Cs^{+3}	76.679	1.70282	Zn_2^{+3}	76.646	1.70278

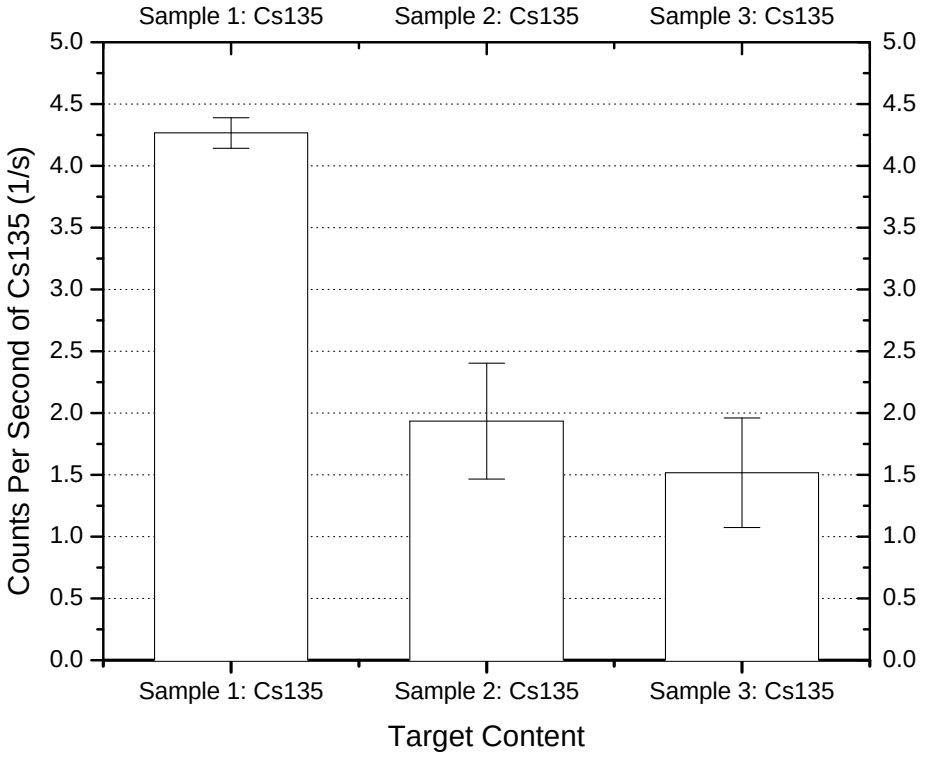

Figure 4.3: ^{135}Cs signal in 3 consecutive samples. The first sample contained ^{135}Cs and the following 2 contained none so the signals in samples 2 and 3 are from cross contamination.

4.4 Reproducibility

A rigorous test for reproducibility of Cs measurement on ISA-AMS was not included in these experiments due to the scarcity of analyte and limited availability of the ISA device.

However, through examination of the data, a qualitative assessment of consistency can be made.

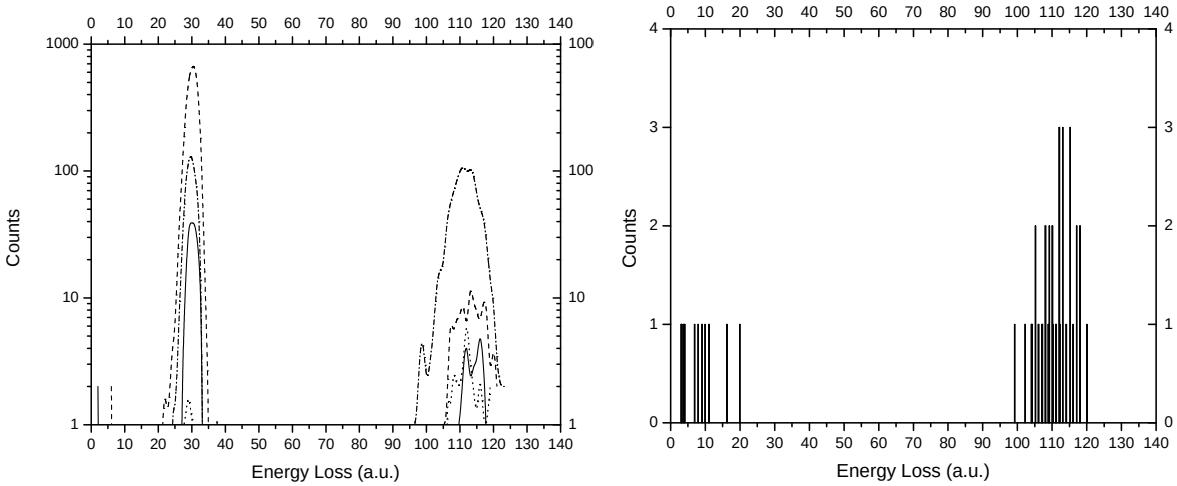

(a) Four different ^{135}Cs measurements (b) Four different ^{134}Cs measurements

Figure 4.4: The GIC spectrum of ^{134}Cs and ^{135}Cs samples with 0.53 Pa of O_2 in the gas cell. These samples contain approximately 1.8×10^{12} atoms of ^{134}Cs and 5.3×10^{13} atoms of ^{135}Cs.

The sequential analysis procedure adjusts the system such that all measured ions will have the same energy as they are measured by the GIC detector. Figure 4.4 demonstrates the consistency of the sequential measurement procedure. Here, eight separate measurements are shown, four of ^{135}Cs and four from ^{134}Cs. Each spectrum lies within the chosen energy range and also displays significant separation from the equal m/z interferences.

Being limited by sample material, targets were created in duplicate rather than triplicate. The results from the analysis of the duplicate targets containing ^{134}Cs and ^{135}Cs can be seen in table 4.6. The values found from this analysis do not agree with the expected value or themselves within statistical error. Therefore, while the ISA-AMS system can consistently detect rare isotopes of Cs, the procedures' ability to reproduce reliable isotope ratios must be developed in future work.

Table 4.6: Ratio of ^{134}Cs/^{135}Cs measurements of duplicate targets. Two measurements were done per target. The expected ratio is the ratio of isotopes added to the target. The results from the first target were not corrected for the Cs memory effect, the second target results were.

Target Content	1st Measurement	2nd Measurement	Expected Ratio
$^{134/135}$Cs	0.46 ± 0.36	0.01 ± 0.01	0.03
$^{134/135}$Cs	0.08 ± 0.03	0.11 ± 0.05	0.03

4.5 Detection Limit and Abundance Sensitivity

The tests performed on the ISA-AMS system provide measurements for the abundance sensitivity of ^{135}Cs. In 200 seconds, 3 counts of ^{135}Cs were obtained (0.015 cps) with a $^{133}Cs^{+3}$ current of 0.056 nA as measured by a FC located just before the final GIC detector. The counts of these two isotopes can be used to calculate the abundance sensitivity of ^{135}Cs/ ^{133}Cs $= (1.3 \pm 1.7) \times 10^{-10}$ which is comparable to the sensitivities reported for TIMS analysis.[1]

It is not clear, however, whether the source of ^{135}Cs counts were truly from the neighbouring ^{133}Cs peak or from source contamination from preceding tests. The latter situation appears more reasonable as initial experiments had demonstrated 0.002 cps of ^{134}Cs from a blank target. Regardless of the source contamination, however, a detection limit of ^{135}Cs can be obtained. The 3σ detection limit of ^{135}Cs measurement on the ISA-AMS system was found to be 6×10^{11} atoms or 132.5 pg of analyte per target.

4.6 Conclusions

These experiments outline the methods by which the detection of ^{135}Cs by AMS was achieved. Cs anion formation remains the limiting factor in Cs analysis with a measured efficiency of 10^{-7}. Including the AMS system transmission efficiency of 1.7% the total efficiency of Cs measurement was found to be 1.7×10^{-9}. A comparison of routine efficiencies can be seen in table 4.7.

Table 4.7: Comparison of different isotope efficiencies on the AMS system.

Element	Efficiency
Iodine	1.2×10^{-2}
Plutonium	1.3×10^{-4}
Carbon	9×10^{-2}
Caesium	1.7×10^{-9}

Using the ISA, all Ba interferences were reduced to 0 counts in 20 minutes with 0.53 pa of O_2 in the reaction cell. Zn dimer interference was easily removed by the increasing of stripper pressure in the tandem accelerator. The remaining interference stems from sample crosstalk in the source environment. The expulsion of large amounts of material at the onset of sputtering is not unique to PbF_2 targets; the process also occurs in Iodine and other targets. For iodine, the expulsion is minimized by gradually increasing the sputtering current on the target, a process known as "conditioning". Doing so preserves the structural integrity of the sample material and improves the lifetime of the target. A similar procedure should be developed for the Cs+PbF_2 targets. Additionally, copper target pieces, due to their superior thermal conductive properties, in lieu of stainless steel, should be tested on the sputter source since this should also reduce residual contamination.

Reproducibility of the system was not tested at length. However, qualitative deductions can be made regarding the data from this initial test. The low count rate and prevailing interferences result in repeated measurements that were not reproducible. Further experimentation should be done to examine the reproducibility of the system once the source cross talk is eliminated.

A summary of the detection limits and abundance sensitivities for each TIMS, ICPMS, and AMS can be seen in table 4.8. The measurements reported here for AMS were collected from targets containing only ^{133}Ca and ^{134}Cs. While the AMS abundance sensitivity matches the order of magnitude reported for TIMS, the detection limit is over 100 times larger than reported for MC-ICPMS. The abundance sensitivity requires further

exploration as the ^{135}Cs measured in these cases may be from source memory effects.

Table 4.8: Comparison of AMS, TIMS, and ICPMS Cs measurement characteristics. [1, 2]

Technique	On-line Ba Suppression	Limit of Detection	^{135}Cs/^{133}Cs
TIMS	N/A	N/A	3×10^{-10}
MC-ICPMS	1×10^{-4}	0.01 pg/mL^{-1}	1×10^{-9}
ISA-AMS	2×10^{-5}	132.5 pg	1.3×10^{-10}

The successful first measurements of ^{135}Cs are an important first step in the advancement of Cs analysis by AMS. By reducing the source memory effects, Cs measurement should report higher reproducibility as well as lower abundance sensitivity and detection limit.

Chapter 5

Caesium-135 Half Life Measurement

5.1 Purpose

The long lived ^{135}Cs isotope has the potential to be a powerful tracing tool and to replace the shorter lived ^{137}Cs in many applications. In order for ^{135}Cs to be an effective tool, however, its half life ($t_{1/2}$) needs to be accurately determined with a high degree of precision.

Currently, two independent studies of the $t_{1/2}$ have been performed, both in 1949. The first, conducted by Sugarman, reported two values: 1.85 and 2.3 Ma with an estimated error of 20%.[22] The value quoted in many tables of isotopes is 2.3Ma. The second measurement was performed by Oak Ridge National Laboratory, which determined the half life to be $2.95 \pm 10\%$Ma.[23] Both of these values were obtained by allowing a known amount of ^{135}Xe to decay and measuring the beta decay from the resulting ^{135}Cs. Beta spectroscopy is the only method of decay measurement since ^{135}Cs is a pure beta emitter.

The uncertainty from these values arises from the difficulty of obtaining pure ^{135}Xe and then accurately measuring the ^{135}Cs decay rate. Additionally, the amount of ^{135}Xe needed to produce a measurable amount of ^{135}Cs is large. A total of 66 curies of ^{135}Xe was used in Sugarman's tests.

Mass spectrometry has proven to be an accurate tool for half life measurements and eliminates the need to handle ^{135}Xe directly.[24] Both thermal ionization mass spectrometry (TIMS) and inductively coupled plasma mass spectrometry (ICPMS) can measure Cs. AMS, however, has the ability to measure lower concentrations of isotopes and, with the addition of an isotope separator for anions (ISA), can eliminate the interferences of ^{134}Ba, ^{135}Ba, and ^{137}Ba. The experiments outlined herein were performed at IsoTrace Laboratory, University of Ottawa, ISA-AMS facility. The purpose of this study was to remeasure the half life of ^{135}Cs using AMS and beta counting.

5.2 Methods

The decay of an atom follows the differential equation for exponential decay:

$$\frac{dN}{dt} = -\lambda N \tag{5.1}$$

Where, N, is the number of atoms in the sample and λ is the decay constant of the atom. This differential equation has a solution of the form:

$$N(t) = N_o e^{-\lambda t} \tag{5.2}$$

By definition $N(t_{1/2}) = N_o/2$. Therefore the decay constant can be found to be:

$$\lambda = \frac{\ln(2)}{t_{1/2}} \tag{5.3}$$

Substituting equation 5.3 into equation 5.1, defining dN/dt as radioactivity, A, and solving for $t_{1/2}$ we get:

$$t_{1/2} = \ln 2 \left(\frac{N}{A}\right) \tag{5.4}$$

Therefore, the measurement of the $t_{1/2}$ of ^{135}Cs can be done in two discrete parts as

represented in equation 5.4. The number of ^{135}Cs atoms in the sample, N, was measured by AMS and the corresponding activity, A, was measured by liquid scintillation counting (LSC). However, since ^{135}Cs is not available as a pure material, this isotope as well as others used in this experiment had to be produced as part of this work.

5.2.1 Isotope Production

Quantities of two separated isotopes were required for this measurement: ^{135}Cs for the half life measurement and ^{134}Cs as a yield tracer and reference material. Yield tracing is a useful technique for determining the amount of a component in a sample. This is accomplished by spiking the analyte, in this case ^{135}Cs, with a known quantity of comparable substance. Ideally, neither the sample of interest nor the spike would contain its counterpart isotope. In AMS this substance is commonly a different isotope of the element of interest. Since ^{135}Cs and ^{137}Cs are both created by nuclear fission in similar amounts and are of interest in AMS Cs measurements, it was determined ^{134}Cs would be the most appropriate yield tracer.

Caesium-134

A sample of ^{134}Cs was produced for these experiments by exposing a sample of Caesium Carbonate (Aldrich AB8824CHM), $^{133}Cs_2CO_3$, to the neutron flux of the Slowpoke reactor at the Royal Military College of Canada for 210s. By exposing a compound to a neutron flux, ϕ, there is a probability, represented by the constituents' neutron cross section, σ, that heavier isotopes will be created. For a given element in the sample, the rate of neutron capture is derived below.

If the losses due to decay of the daughter isotope or its capture of an additional neutron is negligible, the primary activation product due to neutron capture will increase

as:

$$\frac{dN_{A+1}}{dt} = N_A \sigma_A \phi \tag{5.5}$$

$$N_{A+1}(t) = N_A \sigma_A \phi t \tag{5.6}$$

Where A denotes an atomic mass and t is time. When a second neutron is absorbed, the secondary activation product will be produced as follows, using equation 5.6:

$$\frac{dN_{A+2}}{dt} = N_{A+1}(t) \sigma_{A+1} \phi \tag{5.7}$$

$$\frac{dN_{A+2}}{dt} = N_A \sigma_A \sigma_{A+1} \phi^2 t \tag{5.8}$$

$$N_{A+2}(t) = \frac{1}{2} N_A \sigma_A \sigma_{A+1} \phi^2 t^2 \tag{5.9}$$

It was imperative, therefore, that the exposure time be kept to a minimum as ^{135}Cs, the next heaviest isotope, is also created by this process from the ^{134}Cs. The rate of contamination (ratio of ^{135}Cs to ^{134}Cs) given the activation parameters listed in table 5.1 is defined for this system as:

$$\frac{N_{135}}{N_{134}} = \frac{1}{2} \sigma_{134} \phi t \tag{5.10}$$

$$\approx (3.6 \times 10^{-11} \mathrm{s}^{-1}) t \tag{5.11}$$

Table 5.1: The parameters used for the neutron activation of the $^{133}Cs_2CO_3$. [3]

Activation Parameters	
Slowpoke neutron flux	5×10^{11} cm^{-2}s^{-1}
^{133}Cs neutron cross-section	2.9×10^{-23} cm^2
^{134}Cs neutron cross-section	1.4×10^{-22} cm^2
Exposure Time	210 s

A sample of ^{134}Cs was produced with a calculated contamination of approximately 8 ppb ^{135}Cs which was low enough for this application. The resultant gamma spectrum from the irradiation can be seen in figure 5.1.

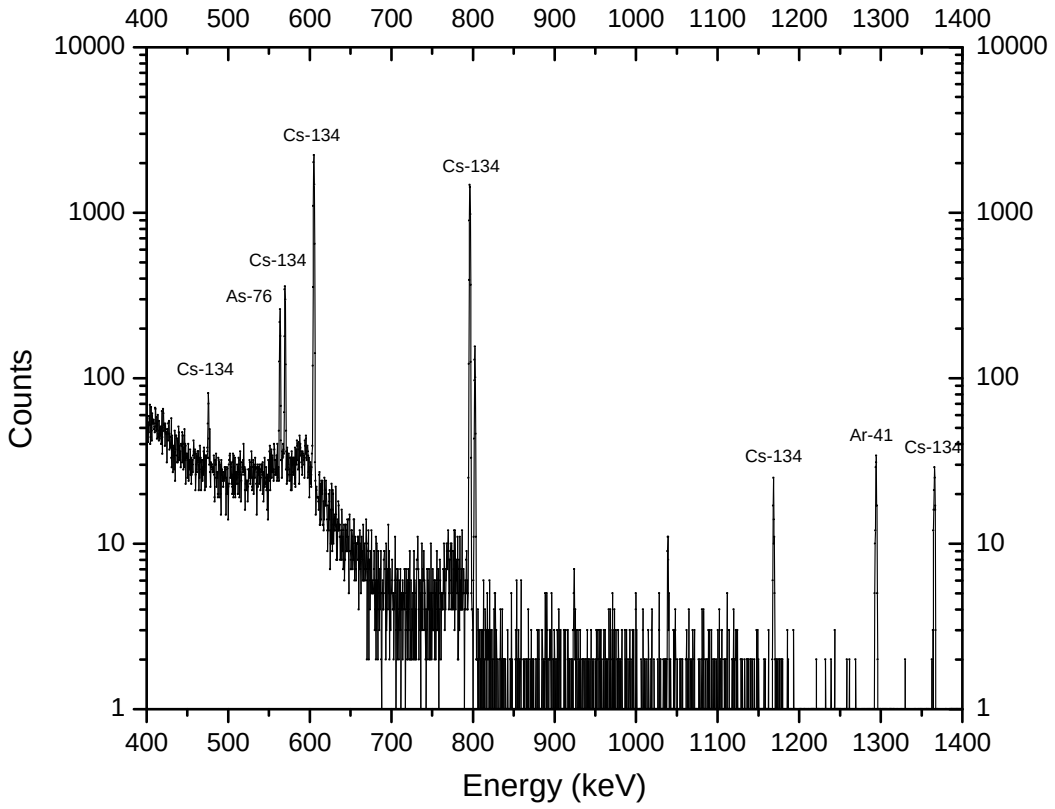

Figure 5.1: Gamma spectrum from the neutron activated Cs_2CO_3.

Caesium-135

^{135}Cs is not available as a separated isotope and its production by neutron capture was not feasible due to ^{134}Cs contamination. Therefore, the ^{135}Cs was obtained through the decay of Xe.

^{135}Xe, which undergoes beta decay to ^{135}Cs ($t_{1/2}$ = 9.14 hr), is created in nuclear reactors during the fission of ^{235}U. In order to preserve the neutron flux of a reactor, the Xe gas has to be extracted, as the large neutron capture cross section of ^{135}Xe causes it to act as a reactor "poison".

A section of Xe exhaust pipe was supplied by Chalk River Laboratories from their xenon gas collection facility. Due to the relatively short half lives of ^{135}Xe and ^{137}Xe, and the stability of ^{134}Xe, any Cs which would have collected in this section of pipe by Xe

decay (equation 5.12) would have been either ^{135}Cs or ^{137}Cs. The pipe was rinsed with distilled water to collect any Cs that had built up in the pipe. The solution was then analyzed by LSC (Perkin Elmer 1220 QUANTULUS Ultra Low Level Liquid Scintillation Spectrometer) to determine its total activity (figure 5.2).

$$\begin{aligned} {}^{135}Xe &\xrightarrow{\beta^- decay} {}^{135}Cs + \beta^- + \nu \qquad (t_{1/2} = 9.14h) \\ {}^{137}Xe &\xrightarrow{\beta^- decay} {}^{137}Cs + \beta^- + \nu \qquad (t_{1/2} = 3.818m) \end{aligned} \tag{5.12}$$

It was determined from the LSC beta spectrum that there was ^{137}Cs and ^{135}Cs in the pipe sample as predicted. Therefore, in order to resolve the partial activity of ^{135}Cs, the activity of ^{137}Cs had to be determined. This was accomplished by gamma counting the pipe sample (figure 5.3). The spectrum also showed that ^{137}Cs was the sole radioactive contaminant.

It was found that ^{137}Cs accounted for 0.39 ± 0.04 Bq per gram of pipe solution. Applying this correction to the LSC measurement, it was found that the activity of ^{135}Cs was:

$$A_{135} = \frac{A_{\text{measured}} - A_{137}\eta_1}{\eta_2} \tag{5.13}$$

$$= \frac{(2.32 \pm 0.02) - (0.39 \pm 0.04)(1.13 \pm 0.01)}{0.84 \pm 0.03} \tag{5.14}$$

$$= 2.2 \pm 0.2 \text{ Bq/g} \tag{5.15}$$

Where η is the efficiency of the LSC for a given decay scheme. As no ^{135}Cs standard exists, ^{45}Ca (Perkin Elmer 12M406B) was used to establish the LSC efficiency, η, for beta particles in the same energy range as those emitted by the decay of ^{135}Cs. The properties of the two decay schemes can be seen in table 5.2.

Table 5.2: Comparison of decay schemes between ^{135}Cs and ^{45}Ca

Isotope	Decay Mode	Branching (%)	Energy (keV)
^{45}Ca	Beta -	100	256.9
^{135}Cs	Beta -	100	268.7

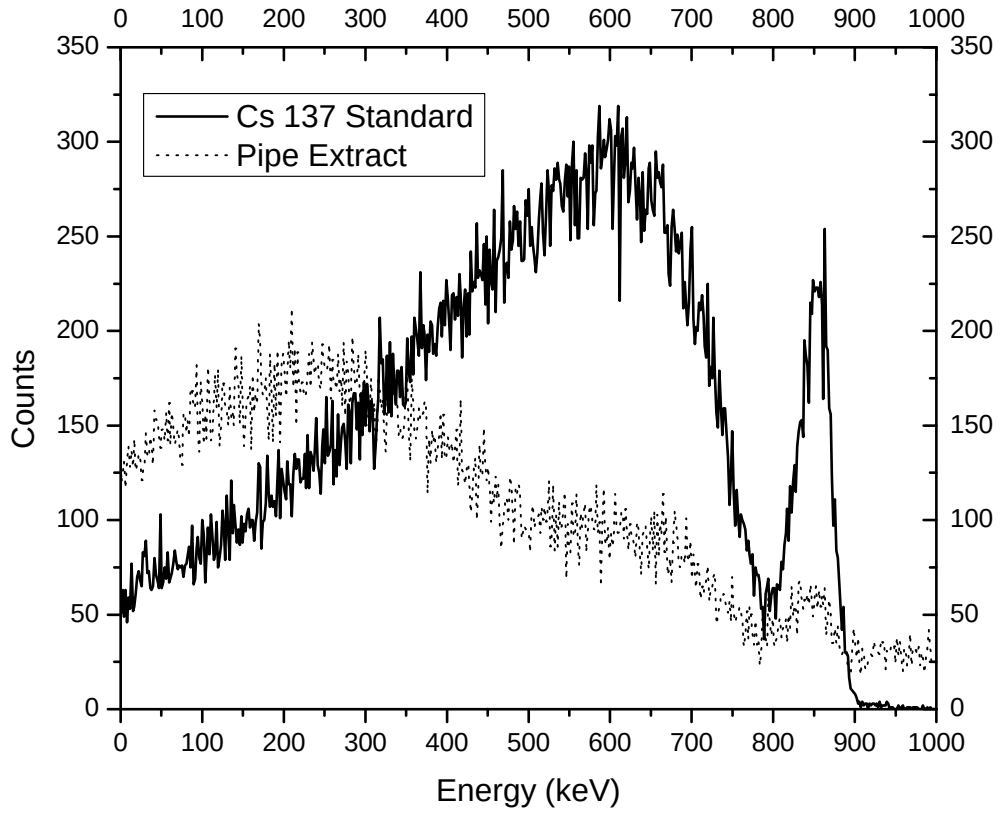

Figure 5.2: Beta decay spectra from the pipe extraction and a ^{137}Cs standard (Amersham CDZ24).

The activity, A_{135}, satisfies half of equation 5.4. The remaining half, the number of ^{135}Cs atoms, N, was found by AMS.

5.2.2 Sample Preparation

To test that the activity of the pipe sample was due only to ^{135}Cs or ^{137}Cs, the Cs was extracted from the solution and analyzed by beta and gamma spectroscopy. This was accomplished using the compound ammonium molybdophosphate (AMP), a resin that selectively binds to Cs. 1g of the ^{135}Cs solution (approximately 1 Bq of Cs) was mixed with 25mg of AMP and shaken by hand for 1 hour. This mixture was placed in a vacuum filtration box and allowed to drip through a glass micro fiber filter (1.6 μm pore size)

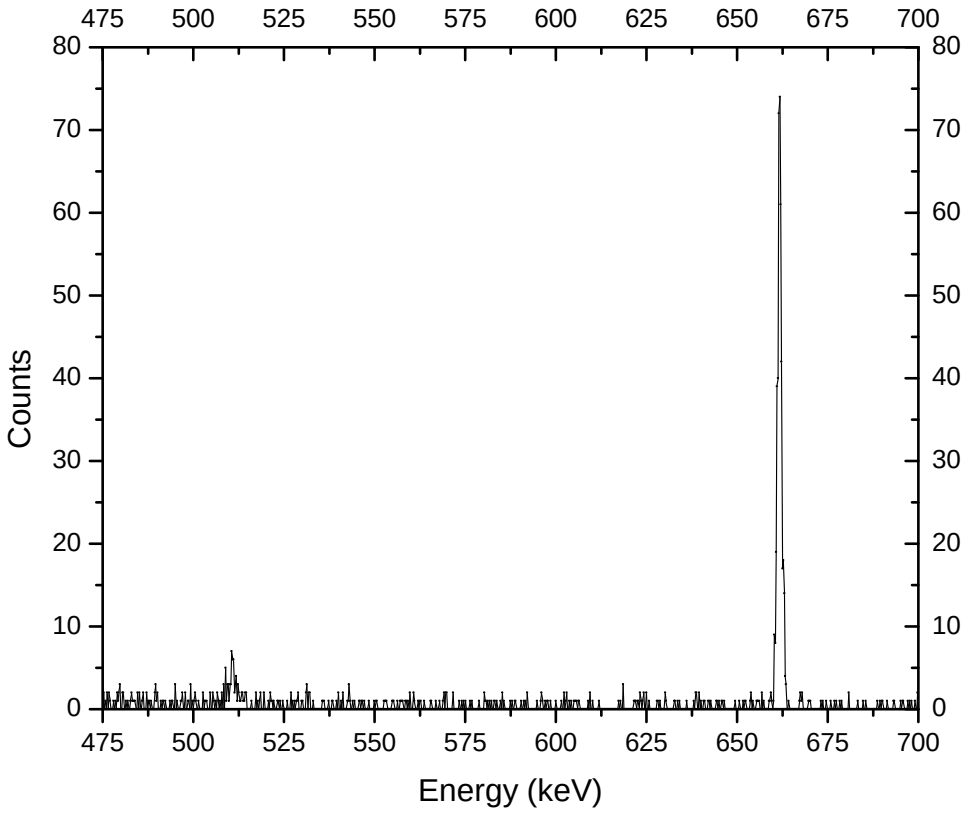

Figure 5.3: Gamma spectrum from the water and dissolved Cs isotopes from the Chalk River Xe exhaust pipe. The small peak at 511 keV is the characteristic annihilation photon. The large peak at 661 keV is the gamma photon from ^{137}Cs decay.

at atmospheric pressure. Once the mixture finished dripping through, the remainder of solution was pulled through the filter by gradually increasing the vacuum box pressure to 15 psi across the filter, leaving only the AMP-Cs complex in the filter paper. To collect any remaining material, the AMP vial was rinsed with 1g of 1% HCl which was subsequently filtered using the same procedure outlined above.

To ensure no loss of analyte in this step, the filtrate was analyzed by gamma and beta spectroscopy. Neither spectrum exhibited activity above background levels. This filtrate was discarded and a new collection vial was added to the column.

The Cs was released from the AMP by adding 1g of 1.5M ammonium hydroxide, an AMP solvent. After pulling the NH_4OH through the filter at 15psi, the filtrate was

shown to contain approximately 80% of the activity of the initial sample aliquot.

Cs atoms do not readily form anions, a characteristic of alkali metal valence electron structures. Therefore, to maximize Cs efficiency, the samples were analyzed as molecular ions, specifically, CsF_2^-. This was accomplished by mixing the Cs samples with PbF_2 prior to ensure conducting and fluorine rich targets. A detailed description of this process can be seen in section 3.2. The samples created for this experiments can be seen in table 4.3.

5.2.3 AMS Procedure

A common practice in AMS is to measure the desired analyte and its abundant isotope concurrently. This practice reduces the need to correct for deviations in the target output current. In the case of Cs however, this is not a suitable practice since the target is bombarded with the abundant isotope, ^{133}Cs. Therefore, the known amount of ^{134}Cs introduced as a yield tracer was also used as a reference isotope to determine the concentration of the ^{135}Cs in the sample. In order to measure this equally rare isotope and monitor the sample for Ba contamination, slow sequential injection of the isotopes of interest was used for the half life measurement.

The mass units that were monitored throughout this experiment include: ^{134}Cs, ^{135}Cs, ^{136}Ba, and ^{137}Ba/Cs. Masses 134 and 135 were measured to determine the amount of ^{135}Cs in the sample while 136 and 137 were observed to ensure consistent suppression of Ba interferences. As a consequence of the instability of the Cs targets and the requirement of sequential measurement, the isotope currents had to be individually normalized. This was accomplished by observing the current of ^{133}Cs in a Faraday cup, located just after the injection magnet, before and after the measurement of an isotope. The value recorded for each isotope was then normalized to the average of the two ^{133}Cs currents, the assumption being that the current decayed linearly with time. While this normalization procedure proved effective for the measurement of Ba in section 3.2, further

experimentation is needed to deduce the relationship between the ^{133}Cs currents and the radioisotopes as a portion of the ^{133}Cs current is due to the sputtering of the sample with ^{133}Cs.

This sequence was completely twice per target. Results from one sequence of measurement can be seen in table 5.3.

Table 5.3: Example ^{135}Cs Half Life Experiment Results.

Sample	134 (counts/s)	135 (counts/s)	136 (counts/s)	137 (counts/s)
^{134}Cs	0.2	0.015	0	0
^{135}Cs	0.096	0.87	0	0.005
$^{134/135}$Cs	0.61	7.6	0	0

From these experiments the concentration of ^{135}Cs in the Chalk River samples could be calculated using the count rates of ^{134}Cs and ^{135}Cs. That is, tracking the counts of ^{134}Cs as a reference, and applying that efficiency to the ^{135}Cs. This estimates the remaining variable in equation 5.4, the ^{135}Cs concentration N.

5.3 Results and Discussion

The values obtained for the half life of ^{135}Cs in these, and previous, experiments can be seen in table 5.4.

Table 5.4: Half lives for ^{135}Cs. This study reports uncertainties to 95% while it is believed the other studies report a 66% uncertainty.

Experiment	Measure Half Life (Ma)	Uncertainty (%)
Sugarmann (1949)	1.85	20
	2.3	20
ORNL (1949)	2.95	10
This study	0.99	42
	0.72	45

The discrepancy and uncertainty in these calculated values emerge from multiple sources. The low number of counts, most significantly of ^{135}Cs, heavily limit the precision of the final measurement. This issue is directly correlated with the limited measurement

lifetime of the targets as well as the low efficiency of Cs ionization. There are many modifications to the target preparation and measurement procedures that require testing to optimize the target lifetime and signal as outlined in section 4.6

Compounding the issue of low count rates is the cross-contamination of ^{134}Cs and ^{135}Cs from one sample to the next. The memory effect needs to be eliminated and/or well characterized so effective corrections can be made. The target preparation adjustments outlined previously should reduce this effect as less material will be ejected into the source environment. While the samples and targets appeared adequate, it is difficult to quantify the amount of ^{135}Cs in the ^{134}Cs reference using decay measurements. However, this can easily be done using AMS as long as there is no residual Cs in the system from previous experiments and the memory effect has been rectified.

Interference from Zn dimers (section 4.3) was not conclusively eliminated from the ^{134}Cs signal. The stripper pressure was increased to ensure the elimination of mass 136. However, referring back to figure 4.2, it can be seen that 134 is the abundant molecule. Therefore, there could have been residual Zn dimer signal in this range, adding more bias to the final measurement. In future, this problem can be eliminated by observing the Zn dimer background prior to the analysis of samples.

Chapter 6

Conclusions

The principle contribution of this thesis is describing the first detection of the ^{135}Cs isotope. Previous experiments have only observed macro-beams of the stable ^{133}Cs isotope. Accomplishing this allows for the development of quantitive techniques which can be used for new applications as well as already established applications involving the radiometric measurement of other Cs isotopes. The 10 main findings of this thesis are summarized below.

1. ^{135}Cs was detected by AMS for the first time. An on-line isobar separator for anions was used to suppress the isobaric interferences of Ba using a selective reaction process.

2. The ISA performed extremely well with O_2 gas in the reaction cell, demonstrating a relative Ba suppression of 2×10^5 while transmitting 25% of the input Cs signal. Suppression in NO_2 gas however, was more efficient at lower pressures (<16 Pa cm), eliminating more Ba and transmitting more Cs.

3. The ISA does not introduce any significant mass dependent fractionation to the AMS system. Without a reaction gas in the ISA, the system was tested for mass dependent fractionation using Ba isotopes. The measured relative abundance of the

six barium isotopes agreed with the natural abundance of the isotopes (correlation 0.991 ± 0.008). No isotope fractionation was detected in the ISA-AMS system over this mass range.

4. The abundance sensitivity of $^{135}Cs/^{133}Cs$ using the IsoTrace ISA-AMS system was 1.3×10^{-10}, a comparable sensitivity to TIMS and a factor of 10 lower than ICPMS.

5. ^{135}Cs concentrations were measured by ISA-AMS using isotope dilution with a known amount of ^{134}Cs. The lower limit of detection of ^{135}Cs in the Isotrace ISA-AMS system was 132.5pg of ^{135}Cs per target; a factor of 10^4 times larger than the lowest limit reported by ICPMS. The detection limit is controlled by the relatively poor efficiency of CsF_2^- negative ion production as well as the Cs memory effect.

6. The production of Cs ion beams was enhanced by accelerating the Cs as CsF_2^- which was produced by fluxing Cs and PbF_2 in HF. The poor efficiency of Cs anion production limits the detection of ^{135}Cs; even with the advancements made during this thesis research. Most targets rarely produced more than 30 nA of Cs current measured after the first injection magnet.

7. Samples of pure ^{134}Cs and $^{135/137}Cs$, were produced by neutron capture and ^{235}U fission, respectively. The ^{135}Cs sample contained 2.2 ± 0.2 Bq/g. This activity was determined by beta counting on a liquid scintillation counter. This is the first time such a large quantity of ^{135}Cs has been produced as a pure isotope.

8. The ^{135}Cs half life was calculated by measuring the activity of ^{135}Cs by LSC and the number of atoms in the sample by ISA-AMS. The number of atoms was measured twice and the half life was calculated to be 0.7 ± 0.3 Ma and 0.99 ± 0.4 Ma. This value is significantly lower than the value reported by previous measurements in 1949.[22, 23]

9. The largest uncertainty arises from the intensity of the Cs memory effect in the

SO110 ion source. It is hypothesized that the memory effect originates from the material discharge that occurs on the initial sputtering of targets that contain PbF_2. A correction was made for the Cs memory bias, however due to the limited data and incomplete understanding of the effect, the adjustment introduced a large uncertainty which was compounded in the detection limit determination and in the half-life calculations.

10. The discharge of ions during the initial sputter introduces additional complications. In order to ensure consistent data, analysis of the target could only begin after the discharge. Consequently, the functional lifetime of the targets was very short, lasting only approximately 30 minutes. The combination of short target lifetime and small Cs currents resulted in the inability to obtain more counts of Cs isotopes and better precision measurements for each isotope.

Chapter 7

Bibliography

[1] T. Lee, K. Teh-Lung, L. Hsiao-Ling, and C. Ju-Chin, "First detection of fallout Cs-135 and potential applications of $^{137}Cs^{135}Cs$ ratios," *Geochimica et Cosmochimica Acta*, vol. 57, no. 14, pp. 3493–3497, 1993.

[2] J. Zheng, K. Tagami, W. Bu, S. Uchida, Y. Watanabe, Y. Kubota, S. Fuma, and S. Ihara, "$^{135}Cs/^{137}Cs$ isotopic ratio as a new tracer of radiocesium released from the Fukushima nuclear accident," *Environmental Science and Technology*, vol. 48, no. 10, pp. 5433–5438, 2014.

[3] S. Mughabghab and N. Holden, *Neutron resonance parameters and thermal cross sections*, ser. Neutron cross sections series. Academic Press, 1981, no. v. 1, pt. 1.

[4] J. Eliades, X. . Zhao, A. E. Litherland, and W. E. Kieser, "On-line ion chemistry for the ams analysis of ^{90}sr and ^{135,137}Cs," *Nuclear Instruments and Methods in Physics Research, Section B: Beam Interactions with Materials and Atoms*, vol. 294, pp. 361–363, 2013.

[5] J. Alary, G. Javahery, W. E. Kieser, X. Zhao, A. Litherland, L. Cousins, and C. Charles, "Isobar separator for anions: Current status." *AM13 Conference Unpublished*, 2014.

[6] H. P. Schwarcz, "Chronometric dating in archaeology: A review," *Accounts of Chemical Research*, vol. 35, no. 8, pp. 637–643, 2002.

[7] S. Epstein and T. Mayeda, "Variation of ^{18}O content of waters from natural sources," *Geochimica et Cosmochimica Acta*, vol. 4, no. 5, pp. 213–224, 1953.

[8] J. S. Becker, "Mass spectrometry of long-lived radionuclides," *Spectrochimica Acta - Part B Atomic Spectroscopy*, vol. 58, no. 10, pp. 1757–1784, 2003.

[9] A. A. Ammann, "Inductively coupled plasma mass spectrometry (icp ms): A versatile tool," *Journal of Mass Spectrometry*, vol. 42, no. 4, pp. 419–427, 2007.

[10] A. E. Litherland, X. L. Zhao, and W. E. Kieser, "Mass spectrometry with accelerators," *Mass spectrometry reviews*, vol. 30, no. 6, pp. 1037–1072, 2011.

[11] R. Hellborg and G. Skog, "Accelerator mass spectrometry," *Mass spectrometry reviews*, vol. 27, no. 5, pp. 398–427, 2008.

[12] M. Liezers, O. T. Farmer III, and M. L. Thomas, "Low level detection of 135Cs and 137Cs in environmental samples by ICP-MS," *Journal of Radioanalytical and Nuclear Chemistry*, vol. 282, no. 1, pp. 309–313, 2009.

[13] D. E. Nelson, R. G. Korteling, and W. R. Stott, "Carbon-14: Direct detection at natural concentrations," *Science*, vol. 198, no. 4316, pp. 507–508, 1977.

[14] X. L. Zhao, A. E. Litherland, J. Eliades, W. E. Kieser, and Q. Liu, "Studies of anions from sputtering i: Survey of MFn -," *Nuclear Instruments and Methods in Physics Research, Section B: Beam Interactions with Materials and Atoms*, vol. 268, no. 7-8, pp. 807–811, 2010.

[15] J. H. Park, B. U. Chang, Y. J. Kim, J. S. Seo, S. W. Choi, and J. Y. Yun, "Determination of low ^{137}Cs concentration in seawater using ammonium 12-

molybdophosphate adsorption and chemical separation method," *Journal of environmental radioactivity*, vol. 99, no. 12, pp. 1815–1818, 2008.

[16] V. F. Taylor, R. D. Evans, and R. J. Cornett, "Preliminary evaluation of ^{135}Cs/^{137}Cs as a forensic tool for identifying source of radioactive contamination," *Journal of environmental radioactivity*, vol. 99, no. 1, pp. 109–118, 2008.

[17] J. Zheng, W. Bu, K. Tagami, Y. Shikamori, K. Nakano, S. Uchida, and N. Ishii, "Determination of ^{135}Cs and ^{135}Cs/^{137}Cs atomic ratio in environmental samples by combining ammonium molybdophosphate (amp)-selective Cs adsorption and ion-exchange chromatographic separation to triple-quadrupole inductively coupled plasma-mass spectrometry," *Analytical Chemistry*, vol. 86, no. 14, pp. 7103–7110, 2014.

[18] J. Eliades, A. E. Litherland, W. E. Kieser, L. Cousins, S. J. Ye, and X. L. Zhao, "Cl/S isobar separation using an on-line reaction cell for ^{36}Cl measurement at low energies," *Nuclear Instruments and Methods in Physics Research, Section B: Beam Interactions with Materials and Atoms*, vol. 268, no. 7-8, pp. 839–842, 2010.

[19] A. E. Litherland, J. Doupé, W. E. Kieser, X. L. Zhao, G. Javaheri, L. Cousins, and I. Tomski, "A negative ion source with isobar selection by chemical reaction cell." Patent US 7 439 498, 10 21, 2008.

[20] X.-L. Zhao, J. Eliades, A. E. Litherland, W. E. Kieser, J. Cornett, and C. R. J. Charles, "On-line HfF5 -/WF5 - separation in an O2-filled radiofrequency quadrupole gas cell," *Rapid Communications in Mass Spectrometry*, vol. 27, no. 24, pp. 2818–2822, 2013.

[21] M. P. Unterweger, D. D. Hoppes, and F. J. Schima, "New and revised half-life measurements results," *Nuclear Inst.and Methods in Physics Research, A*, vol. 312, no. 1-2, pp. 349–352, 1992.

[22] N. Sugarman, "Characteristics of the fission product ^{135}Cs," *Physical Review*, vol. 75, no. 10, pp. 1473–1476, 1949.

[23] H. Zeldes, A. Brosi, G. Parker, G. Herbert, and G. Creek, "Characterization of ^{135}Cs," *Oak Ridge National Laboratory Progress Report*, vol. 286, pp. 48–52, 1949.

[24] G. Jörg, Y. Amelin, K. Kossert, and C. Lierse v. Gostomski, "Precise and direct determination of the half-life of ^{41}ca," *Geochimica et Cosmochimica Acta*, vol. 88, pp. 51–65, 2012.

[25] O. Masson *et al.*, "Tracking of airborne radionuclides from the damaged fukushima dai-ichi nuclear reactors by european networks," *Environmental Science and Technology*, vol. 45, no. 18, pp. 7670–7677, 2011.

[26] D. E. Walling and H. Qingping, "Interpretation of caesium-137 profiles in lacustrine and other sediments: the role of catchment-derived inputs," *Hydrobiologia*, vol. 235-236, pp. 219–230, 1992.

[27] J. A. Luque and R. Juliá, "Lake sediment response to land-use and climate change during the last 1000 years in the oligotrophic Lake Sanabria (northwest of iberian peninsula)," *Sedimentary Geology*, vol. 148, no. 1-2, pp. 343–355, 2002.

[28] D. Lariviere, V. F. Taylor, R. D. Evans, and R. J. Cornett, "Radionuclide determination in environmental samples by inductively coupled plasma mass spectrometry," *Spectrochimica Acta - Part B Atomic Spectroscopy*, vol. 61, no. 8, pp. 877–904, 2006.

[29] J. Lachner, M. Martschini, A. Priller, P. Steier, and R. Golser, "Development towards detection of ^{135}Cs at vera." *AM13 Conference Unpublished*, 2014.